

HAMILTONIAN VS STABILITY IN ALTERNATIVE THEORIES OF GRAVITY^a

G. ESPOSITO-FARESE

*Sorbonne Université, CNRS, UMR7095, Institut d'Astrophysique de Paris,
G_RεCO, 98bis boulevard Arago, F-75014 Paris, France*

When a Hamiltonian density is bounded by below, we know that the lowest-energy state must be stable. One is often tempted to reverse the theorem and therefore believe that an unbounded Hamiltonian density always implies an instability. The main purpose of this presentation (which summarizes my work^{1,2} with E. Babichev, C. Charmousis and A. Lehébel) is to pedagogically explain why this is erroneous. Stability is indeed a coordinate-independent property, whereas the Hamiltonian density does depend on the choice of coordinates. In alternative theories of gravity, like k-essence or Horndeski theories, the correct stability criterion is a subtler version of the well-known “Weak Energy Condition” of general relativity. As an illustration, this criterion is applied to an exact Schwarzschild-de Sitter solution of a Horndeski theory, which is found to be stable for a given range of its parameters, contrary to a claim in the literature.

1 Introduction

It is well-known that any logical implication such as $(A \Rightarrow B)$ may also be rewritten as its contrapositive $(\neg B \Rightarrow \neg A)$, but that its *inverse* $(\neg A \Rightarrow \neg B)$ is generally not true —unless the initial implication was actually an equivalence. It happens that several recent works in theoretical physics have used such an erroneous inversion of a standard theorem about stability. The correct theorem tells us that if a Hamiltonian density is bounded by below, then the lowest-energy state is stable. Indeed, imagine a Hamiltonian having the shape of a U: If the solution corresponds to its minimum, it is impossible to move away without violating the conservation of energy. One may be tempted to inverse the statement by claiming that “a Hamiltonian density which is unbounded from below always imply an instability”. We shall underline why this is erroneous, although many physicists intuitively believe so, probably guided by their experience with ghost degrees of freedom. Of course, not all solutions are stable, otherwise the above standard theorem would not have any interest. In particular, ghosts do lead to deadly instabilities. But we shall see that stable solutions may sometimes correspond to a Hamiltonian density which is unbounded from below. Actually, this is rather trivial once it is understood, but we believe it is important to be underlined, as this changes some conclusions of recent papers about the stability of specific solutions. Let us for instance mention a series of technically excellent works^{3,4,5,6} whose calculations are highly non-trivial and correct, but which unfortunately use the above erroneous “inverse” argument. They compute the Hamiltonian of perturbations around a given background solution, and impose it to be bounded by below. Of course, all the stable cases that they report are indeed (perturbatively) stable, because of the standard theorem recalled above. But they may be discarding other stable cases, which do not satisfy their requirement of a bounded-by-below Hamiltonian. As an example, the first of these references³ claims that a hairy black-hole solution of a given Horndeski theory is *always* unstable, whereas we shall see in Sec. 3 below that it is stable for a given range of the theory parameters.^{1,2} Let us start in Sec. 2 with a discussion of the indirect relation between Hamiltonian and stability.

^aContribution to the 2019 Gravitation session of the 54th Rencontres de Moriond.

2 Stability in presence of several causal cones

2.1 Causal cones and Hamiltonian

Although our discussion is quite general, as this will become clear after having understood it, let us focus for simplicity on *perturbative* stability around a given background, and also only on kinetic terms, as this is where subtleties are hidden. In alternative theories of gravity, there generically exist different causal cones for the various propagating degrees of freedom. The simplest example is k-essence, whose Lagrangian reads $\mathcal{L} = -\frac{1}{2}f(X)$, where $X \equiv g^{\mu\nu}\partial_\mu\varphi\partial_\nu\varphi$ would be the standard kinetic term for a scalar field φ , and f is a function specifying the theory. [We choose the mostly-plus signature convention for the metric $g_{\mu\nu}$.] Let us write $\varphi = \bar{\varphi} + \chi$, where $\bar{\varphi}$ denotes the background solution and χ a small perturbation. Then the second-order expansion of the Lagrangian reads $\mathcal{L}_2 = -\mathcal{G}^{\mu\nu}\partial_\mu\chi\partial_\nu\chi$, where^{7,8,9,10,11,12}

$$\mathcal{G}^{\mu\nu} = f'(\bar{X})g^{\mu\nu} + 2f''(\bar{X})\nabla^\mu\bar{\varphi}\nabla^\nu\bar{\varphi} \quad (1)$$

depends on the first and second derivatives of function f with respect to its argument \bar{X} , and plays the role of an effective metric in which the spin-0 degree of freedom χ propagates. When the background gradient $\nabla^\mu\bar{\varphi}$ does not vanish, the last term of Eq. 1 implies that null directions with respect to $\mathcal{G}^{\mu\nu}$ are not null with respect to $g^{\mu\nu}$ and reciprocally. This corresponds to panel (b) of Fig. 1 when $f'' < 0$, or to panel (c) when $f'' > 0$.

The difficulties arise when one performs a boost with a large enough velocity: Panel (b) is transformed into (a), in which the time axis gets out of the scalar (dashed blue) causal cone, and panel (c) becomes (d), where the spatial x axis enters the scalar cone, on the contrary.^b This causes the Hamiltonian density

$$\mathcal{H}_2 = -\mathcal{G}^{00}\dot{\chi}^2 + \mathcal{G}^{ij}\partial_i\chi\partial_j\chi \quad (2)$$

not to be bounded by below any longer. Indeed, let us denote as $\mathcal{G}_{\mu\nu}$ the *inverse* of the effective metric $\mathcal{G}^{\mu\nu}$ (beware not to confuse it with $g_{\mu\lambda}g_{\nu\rho}\mathcal{G}^{\lambda\rho}$). In the (t, x) subspace of Fig. 1, it reads

$$\begin{pmatrix} \mathcal{G}_{00} & \mathcal{G}_{0x} \\ \mathcal{G}_{0x} & \mathcal{G}_{xx} \end{pmatrix} = \begin{pmatrix} \mathcal{G}^{xx} & -\mathcal{G}^{0x} \\ -\mathcal{G}^{0x} & \mathcal{G}^{00} \end{pmatrix} / D, \quad (3)$$

where the determinant $D \equiv \mathcal{G}^{00}\mathcal{G}^{xx} - (\mathcal{G}^{0x})^2$ must be strictly negative for this effective metric to define a cone (and thereby hyperbolic field equations). In the situation of panel (a) of Fig. 1, the time coordinate is spacelike with respect to the scalar (dashed blue) causal cone, therefore $\mathcal{G}_{00} dx^0 dx^0 > 0$. Because of Eq. 3, this implies $\mathcal{G}^{xx} < 0$. Similarly, in the situation of panel (d), the spatial x axis is timelike with respect to the scalar causal cone, therefore $\mathcal{G}_{xx} dx dx < 0$, which implies $\mathcal{G}^{00} > 0$ from Eq. 3. In both cases, we thus find that the Hamiltonian density, Eq. 2, contains a term, either $\mathcal{G}^{xx}(\partial_x\chi)^2$ or $-\mathcal{G}^{00}\dot{\chi}^2$, which can become infinitely negative.

On the other hand, the Hamiltonian density, Eq. 2, is positive in situations corresponding to panels (b) or (c), because the time axis is timelike and the x axis spacelike with respect to the scalar causal cone, therefore $\mathcal{G}^{xx} > 0$ and $\mathcal{G}^{00} < 0$. This implies that the solution is perturbatively stable, because of the standard theorem recalled at the beginning of the Introduction: It cannot decay toward another state without violating energy conservation. Since panels (a) and (d) correspond to strictly the *same* solutions as (b) and (c), merely seen by a moving observer,

^bNote that although one characteristic goes backwards in time in panel (d) of Fig. 1, causality is anyway preserved, as was discussed in detail more than a decade ago.^{9,10,11,12} If the scalar cone never totally opens, i.e., that its exterior exists everywhere, then one may foliate the full spacetime with hypersurfaces which are spacelike with respect to both $\mathcal{G}^{\mu\nu}$ and $g^{\mu\nu}$, and it is impossible to influence one's past without assuming a non-trivial topology. The only subtlety with panel (d) is that one is not allowed to use the $t = 0$ hypersurface as a Cauchy surface, since it is not spacelike with respect to the scalar causal cone. The data for the scalar perturbation χ are thus obviously constrained on this $t = 0$ hypersurface.

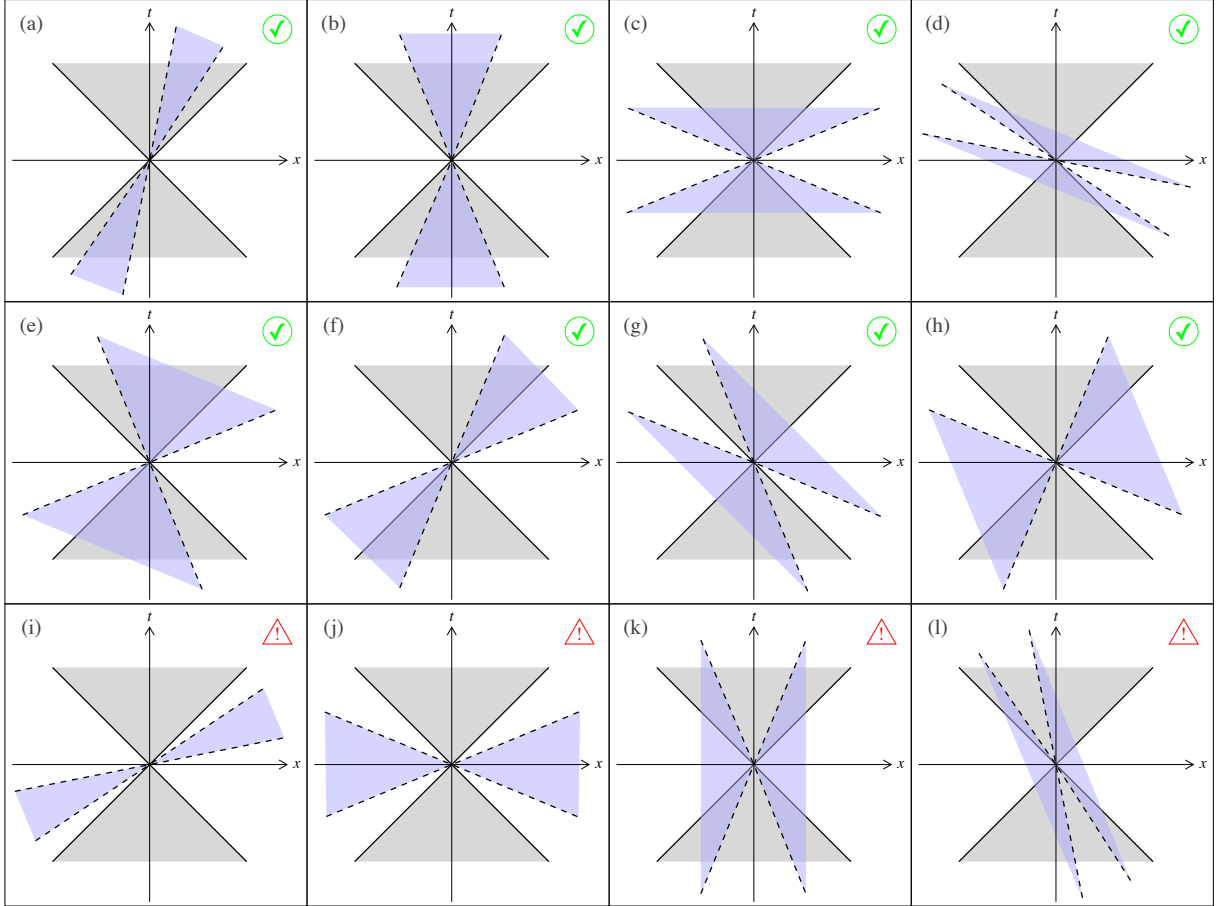


Figure 1 – Possible relative orientations of two causal cones, in a coordinate system such that the grey cone with solid lines appears at $\pm 45^\circ$. We do not plot the equivalent configurations exchanging left and right, and do not consider the limiting cases where some characteristics coincide. In our discussion of k-essence in Sec. 2.1, we assume that the grey cone is defined by $g^{\mu\nu}$, while the dashed (blue) one is defined by the effective metric $\mathcal{G}^{\mu\nu}$ in which spin-0 degrees of freedom propagate.

they must therefore also describe stable cases, in spite of the unboundedness by below of the Hamiltonian.

Before explaining the deep reason why such cases are indeed stable, in Sec. 2.2 below, we may already draw conclusions from our argument above: If there exists a coordinate system in which the Hamiltonian density is bounded by below, then the standard theorem implies that the solution is stable—even if it is unbounded by below in other coordinate systems. In terms of the spacetime diagrams of Fig. 1, stability means thus that all causal cones should have a common interior (intersection of the grey and blue cones), where a new time axis may be chosen, and also a common exterior (white region in Fig. 1), where a new spatial x axis may be defined. As discussed above, panels (a) and (b) are thus equivalent, as well as (c) and (d), and they all describe stable cases.

The same reasoning shows that all four panels (e)–(h) also correspond to stable solutions: There always exists a coordinate system (not necessarily obtained by a mere boost) bringing them to the case of panel (e), where the time axis is timelike with respect to all causal cones, and the x axis is spacelike, so that the Hamiltonian density, Eq. 2, becomes positive. This second row of Fig. 1 is interesting for two reasons. First, it illustrates the unusual situation in which the two metrics $g^{\mu\nu}$ and $\mathcal{G}^{\mu\nu}$ cannot be simultaneously diagonalized. We know that two quadratic forms can always be simultaneously diagonalized when at least one of them is positive (or negative) definite, but here both metrics have a hyperbolic signature. In this second row, one of the scalar’s characteristics is within the grey cone, and the other one outside it,

therefore no coordinate transformation can bring them to a symmetric configuration like those of panels (b), (c), (j) or (k). The second instructive point is about panel (h): The time axis is spacelike with respect to the scalar causal cone, while the x axis is timelike with respect to this blue cone. Therefore, the contribution of the scalar degree of freedom to the Hamiltonian density, Eq. 2, is *always* negative in this coordinate system. On the other hand, usual matter fields minimally coupled to $g_{\mu\nu}$ give a positive contribution to the Hamiltonian density, since the grey causal cone has a standard orientation with respect to the coordinate axes. Panel (h) corresponds thus to a situation in which the Hamiltonian density is the sum of a negative (scalar) contribution and a positive (matter) one. One may thus be tempted to naively conclude that this solution should decay into an infinite number of negative-energy scalar modes, compensated by an infinite number of positive-energy matter ones. However, there exists another coordinate system, in which the time axis is chosen in the intersection of the grey and blue cones, and the x axis in the white region outside both of them, such that the total Hamiltonian (of matter plus the scalar field) is bounded by below. The standard theorem therefore implies that this solution must be stable, and we shall better understand why in Sec. 2.2.

The last row of Fig. 1, panels (i)–(l), describes the unstable cases. The two metrics can be simultaneously diagonalized by a coordinate change, transforming panel (i) into (j) and (l) into (k). But in the (t, x) subspace of this figure, panels (j) and (k) correspond to *opposite* signatures of the two metrics $g^{\mu\nu}$ and $\mathcal{G}^{\mu\nu}$: One is $(-, +)$ and the second $(+, -)$. Therefore, the scalar degree of freedom behaves as a ghost in this (t, x) subspace, and the solution will indeed decay into an infinite amount of negative-energy scalar modes compensated by positive-energy matter ones. For this last row of Fig. 1, there does not exist *any* coordinate system in which the total Hamiltonian density (of matter plus the scalar field) is bounded by below.

2.2 Conserved quantities

Let us now explain why some solutions may be stable in spite of their unbounded Hamiltonian density—including in the worst case of panel (h). The reason is that energy is not the only conserved quantity. Since Lagrangian \mathcal{L}_2 (defined above Eq. 1) is a scalar, it is invariant under time and space translations, therefore there exist four Noether currents

$$-T_\mu^\nu \equiv \frac{\delta \mathcal{L}_2}{\delta(\partial_\nu \chi)} \partial_\mu \chi - \delta_\mu^\nu \mathcal{L}_2, \quad (4)$$

where μ specifies which current is considered and ν denotes its components. When integrating their conservation equation $\partial_0 T_\mu^0 + \partial_i T_\mu^i = 0$ (here written in flat spacetime to simplify) over a large spatial volume V containing the whole physical system, the spatial derivatives become vanishing boundary terms, and one gets the standard conservation laws for total energy and momentum, $\partial_t P_\mu = 0$, with $P_\mu \equiv -\iiint_V T_\mu^0 d^3x$. For $\mu = 0$, the energy density $-T_0^0$ coincides with Eq. (2). As shown above, even if one starts from a positive value of $-T_0^0$ in a coordinate system corresponding to panels (b), (c) or (e) of Fig. 1, the total energy $P'_0 = (\partial x^\mu / \partial x'^0) P_\mu$ may become negative in another coordinate system—corresponding to panels (a), (d), (f), (g) or (h). But all four quantities P'_λ are anyway conserved, in this new coordinate system, and it happens that there exists a linear combination of them which is bounded by below. Indeed, $P_0 = (\partial x'^\lambda / \partial x^0) P'_\lambda$ gives precisely the positive energy which was computed in the initial coordinate system of panels (b), (c) or (e). In conclusion, when the Hamiltonian density is not bounded by below, there may anyway exist a linear combination of the four conserved Noether currents which is bounded by below, and its existence suffices to ensure stability—for the same reason as in the standard theorem recalled at the beginning of the Introduction. This conserved and bounded-by-below quantity actually coincides with the Hamiltonian computed in a “good” coordinate system, such that time is timelike and space spacelike with respect to all causal cones, consistently with our conclusions of Sec. 2.1.

2.3 Stability criterion

The eight stable cases (a)–(h) of Fig. 1 may be translated as conditions on the components of the effective metric $\mathcal{G}^{\mu\nu}$. In the (t, x) subspace of this figure, and in a coordinate system such that $g_{\mu\nu} = \text{diag}(-1, 1)$, one finds that stability requires

$$D \equiv \mathcal{G}^{00}\mathcal{G}^{xx} - (\mathcal{G}^{0x})^2 < 0 \quad (\text{hyperbolicity}), \quad (5)$$

$$\mathcal{G}^{00} < \mathcal{G}^{xx} \quad \text{and/or} \quad |\mathcal{G}^{00} + \mathcal{G}^{xx}| < 2|\mathcal{G}^{0x}| \quad (\text{existence of consistent time and space coordinates}). \quad (6)$$

This means that the off-diagonal component \mathcal{G}^{0x} should be large enough. For instance, if $0 < \mathcal{G}^{00} < \mathcal{G}^{xx}$, then Eq. 5 implies that \mathcal{G}^{0x} is large enough to ensure the existence of a coordinate system in which time is timelike and space spacelike with respect to all causal cones. But if $0 < \mathcal{G}^{xx} < \mathcal{G}^{00}$, then Eq. 6 implies that $|\mathcal{G}^{0x}|$ must be even larger, namely greater than the arithmetical mean $\frac{1}{2}|\mathcal{G}^{00} + \mathcal{G}^{xx}|$, known to be always greater than the geometrical mean $\sqrt{\mathcal{G}^{00}\mathcal{G}^{xx}}$ entering Eq. 5. By contrast, the positivity of the Hamiltonian, Eq. 2, would need $\mathcal{G}^{00} < 0$ and $\mathcal{G}^{xx} > 0$, which is much more restrictive than Eqs. 5–6 above, and does not depend at all on \mathcal{G}^{0x} . This shows that some stable solutions may have been wrongly discarded in the recent literature.^{3,4,5,6} Actually, some of these references chose to replace the positivity of the Hamiltonian by the “necessary” condition $\mathcal{G}^{00}\mathcal{G}^{xx} < 0$. But contrary to the hyperbolicity condition, Eq. 5, this inequality is obviously coordinate-dependent: As illustrated in Sec. 2.1, different observers may find opposite signs for the product $\mathcal{G}^{00}\mathcal{G}^{xx}$, whereas stability is a physical statement which should be coordinate-independent.

To simplify, the second line of the above stability conditions, Eq. 6, has been written in a specific coordinate system such that $g_{\mu\nu} = \text{diag}(-1, 1)$. It may of course be generalized to an arbitrary coordinate system, but it is more useful to express it in a covariant way. We found² that the necessary and sufficient conditions for stability are the following. First, all metrics (here $g_{\mu\nu}$ and $\mathcal{G}_{\mu\nu}$, but there may exist more for other degrees of freedom) should be of hyperbolic mostly-plus signature. This generalizes Eq. 5 above. Second, there should exist at least one contravariant vector U^μ and one covariant vector u_μ (generically not related to each other by raising or lowering their index with any of the metrics) such that

$$g_{\mu\nu}U^\mu U^\nu < 0, \quad \mathcal{G}_{\mu\nu}U^\mu U^\nu < 0, \quad \dots \quad (7)$$

$$g^{\mu\nu}u_\mu u_\nu < 0, \quad \mathcal{G}^{\mu\nu}u_\mu u_\nu < 0, \quad \dots \quad (8)$$

for all metrics (where we recall that $\mathcal{G}_{\mu\nu}$ denotes the *inverse* of $\mathcal{G}^{\mu\nu}$). Equation 7 implies the existence of a common interior to all causal cones, where a “good” time axis may be chosen, namely dx^0 in the direction of U^μ . Equation 8 expresses the existence of a spatial hypersurface exterior to all causal cones, defined by $u_\mu dx^\mu = 0$, where “good” spatial coordinates may be chosen. Finally, the positivity of the Hamiltonian density in such a good coordinate system may be covariantly written as

$$T_\mu^\nu U^\mu u_\nu \geq 0, \quad (9)$$

where T_μ^ν denotes the total energy-momentum tensor for all fields.

Equations 7–9 actually generalize the “Weak Energy Condition” of general relativity. When there exists only one metric $g_{\mu\nu}$ to which all fields are minimally coupled, and thereby a single causal cone for all degrees of freedom, one may of course choose $u_\mu = g_{\mu\nu}U^\nu$, and Eq. 9 becomes the standard condition $T_{\mu\nu}U^\mu U^\nu \geq 0$ for any timelike vector U^μ . Note that even in general relativity, the single causal cone defined by $g_{\mu\nu}$ may be oriented like the dashed blue cones of Fig. 1. For instance, in the interior of a Schwarzschild black hole, Schwarzschild coordinates define the time axis outside the causal cone —similarly to the blue cone of panels (j) or (k). More generally, *any* coordinate system is allowed in general relativity, even if the time axis is outside the causal cone and/or some spatial axes within it. In such cases, it is well-known that

the Hamiltonian density $-T_0^0$ is not positive, but that the correct stability criterion involves the contraction $T_{\mu\nu}U^\mu U^\nu$ with a timelike vector U^μ (i.e., such that $g_{\mu\nu}U^\mu U^\nu < 0$). Our conclusions above are straightforward generalizations: One should never trust coordinate-dependent reasonings, and the Hamiltonian density does depend on the coordinate system, since it is not a scalar quantity.

As an example, let us quote the theoretical constraints imposed by the above stability conditions, Eqs. 5-6 or Eqs. 7-9, on k-essence theories (defined above Eq. 1). One recovers those which have been derived several times in the literature with various viewpoints.^{7,8,9,10,11,12} One needs $f'(X) > 0$ and $2Xf''(X) + f'(X) > 0$, whatever the direction of the gradient $\nabla^\mu\varphi$ (timelike, spacelike or null). This imposes in particular that there exists a common spacelike exterior to both causal cones (defined by $g_{\mu\nu}$ and $\mathcal{G}_{\mu\nu}$), where one may specify initial data. Note that there is no constraint on $f''(X)$ alone, and therefore that both infraluminal [panels (a) or (b) of Fig. 1] and superluminal cases [panels (c) or (d)] are allowed.

3 Stable black hole in a Horndeski theory

A better illustration of the above stability criterion is provided by a simple Horndeski theory,¹³ defined by the action

$$S = \int \left[\zeta(R - 2\Lambda_{\text{bare}}) - \eta(\partial_\mu\varphi)^2 + \beta G^{\mu\nu}\partial_\mu\varphi\partial_\nu\varphi \right] \sqrt{-g} d^4x, \quad (10)$$

where R is the scalar curvature of the metric $g_{\mu\nu}$ (to which all matter fields are assumed to be minimally coupled), $G^{\mu\nu}$ is its Einstein tensor (not to be confused with the effective metric $\mathcal{G}^{\mu\nu}$ of Eq. 1), Λ_{bare} denotes a bare cosmological constant, and ζ, η, β are constant parameters. This theory admits an exact Schwarzschild-de Sitter solution of the form¹⁴

$$ds^2 = -A(r) dt^2 + \frac{dr^2}{A(r)} + r^2 (d\theta^2 + \sin^2\theta d\phi^2), \quad (11)$$

$$A(r) = 1 - \frac{2Gm}{r} - \frac{\Lambda_{\text{eff}}}{3} r^2, \quad \text{with } \Lambda_{\text{eff}} = -\frac{\eta}{\beta}, \quad (12)$$

$$\varphi = q \left[t - \int \frac{\sqrt{1-A(r)}}{A(r)} dr \right], \quad \text{with } q^2 = \frac{\eta + \beta\Lambda_{\text{bare}}}{\eta\beta} \zeta. \quad (13)$$

Its interesting property is that the observable cosmological constant Λ_{eff} , entering the line element ds^2 through Eq. 12, is not the bare one of action Eq. 10, but an effective one which may be small enough to be consistent with observation even if Λ_{bare} is huge (for instance the square of the Planck mass, or even larger). In the present model, Λ_{eff} does not even depend at all on Λ_{bare} , but only on the two kinetic terms defining the dynamics of the scalar field φ in Eq. 10. This is a particularly nice example of what is called “self-tuning”:^c The scalar field automatically adjusts itself so that its energy-momentum tensor $T_{\mu\nu}$ almost perfectly balances the vacuum energy $\Lambda_{\text{bare}} g_{\mu\nu}$ entering Einstein’s equations, in order to let a tiny observable one $\Lambda_{\text{eff}} g_{\mu\nu}$.

To analyze the stability of such a solution, we need to extract the effective metrics in which spin-0 and spin-2 perturbations propagate. The most efficient method would be to find a change of variables diagonalizing their kinetic terms, i.e., what is called the “Einstein frame”. The procedure is well-known for standard (Jordan-Fierz-Brans-Dicke) scalar-tensor theories or $f(R)$ theories, and this was also achieved for the quadratic plus cubic Galileon model,¹⁶ but we did not find any covariant change of variables separating the degrees of freedom in the present theory. We have thus studied perturbations by decomposing them on spherical harmonics.^{3,1,2}

^cIt was later shown¹⁵ that such a self-tuning can be achieved in basically *all* Horndeski and beyond-Horndeski theories, provided the action contains at least two of the six possible terms defining the scalar’s dynamics.

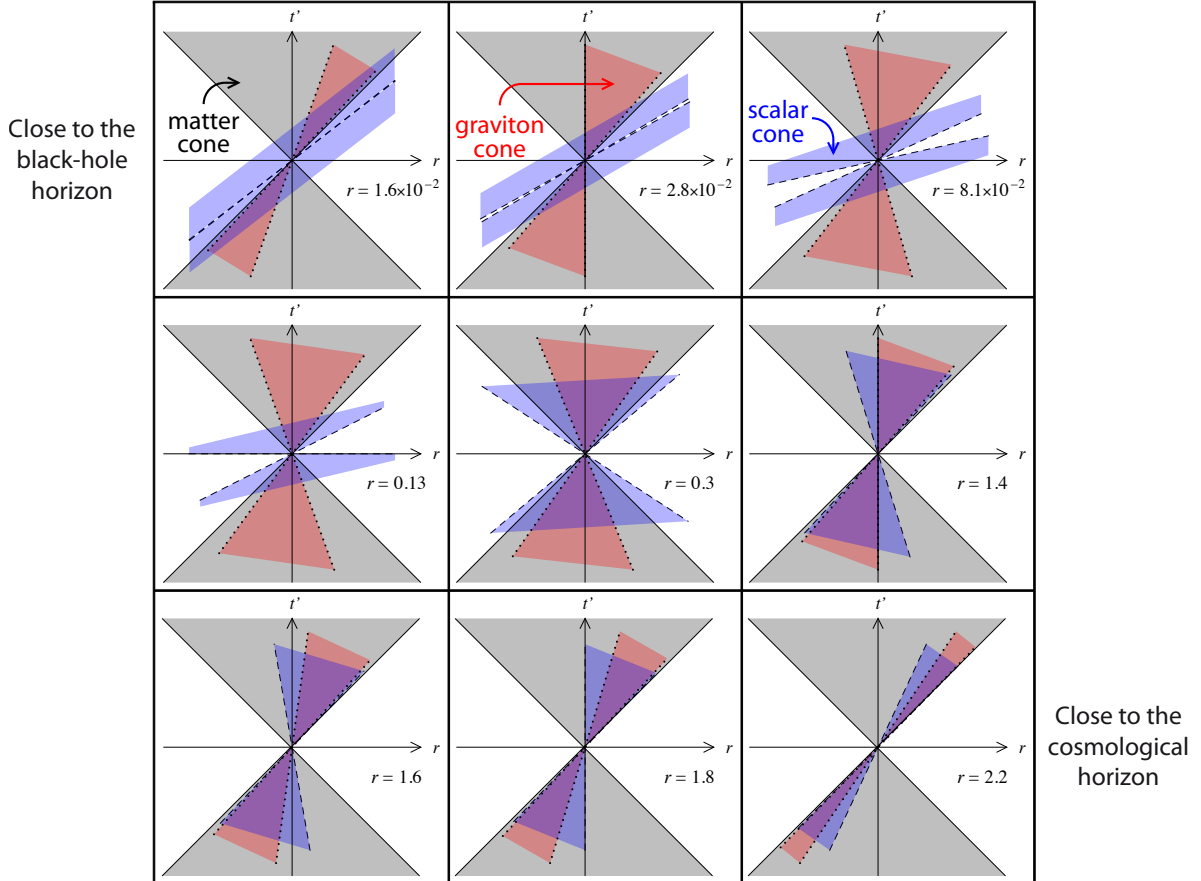


Figure 2 – Matter (solid grey), graviton (dotted red) and scalar (dashed blue) causal cones in the exact Schwarzschild-de Sitter solution of Eqs. 11–13, for parameters $\beta = -1$ and $\zeta = \Lambda_{\text{bare}} = 2\eta = 1$ in Planck units. Static Schwarzschild coordinates are used, but the time axis has been rescaled so that the grey cone (defined by $g_{\mu\nu}$) appears at $\pm 45^\circ$. The successive panels correspond to situations from close to the black-hole horizon at the top-left, to close to the cosmological horizon at the bottom-right.

Odd-parity perturbations necessarily correspond to the spin-2 degree of freedom, and we fully agree with the analytical results previously derived in the literature.³ However, the conclusion of this reference was that this solution is always unstable, because the product $\mathcal{G}^{00}\mathcal{G}^{rr}$ becomes positive close enough to the black-hole horizon (see our discussion below Eq. 6). Instead of writing a heavy analytical expression for this product, let us plot the causal cones in Fig. 2. The dotted red ones represent the graviton causal cone we are presently discussing. The fact that $\mathcal{G}^{00}\mathcal{G}^{rr}$ becomes positive is vividly illustrated by the top-left panel: The time axis gets out of this red cone. However, it is also clear that one may choose another time axis within this graviton causal cone (which happens to be itself inside the matter causal cone^d), and the perturbation Hamiltonian will become positive in this new coordinate system. Therefore, there is actually no instability caused by the gravitons. It is also easy to check on Fig. 2 that at any distance from the black hole, there always exist a common interior and a common exterior to the matter and graviton causal cones. Actually, note that the graviton cone is also very tilted near the cosmological horizon (bottom-right panel). Therefore, the same argument as the literature³ about the sign of $\mathcal{G}^{00}\mathcal{G}^{rr}$ would have also concluded that the solution must be unstable. But this is again a coordinate artifact, caused here by the static Schwarzschild coordinates used in this figure. If one used Friedmann-Lemaître-Robertson-Walker coordinates instead, the red (graviton) cone would remain thinner than the grey (matter) one, close to the cosmological

^dSee our published articles^{1,2} for a modification (in the beyond-Horndeski class of theories) of the model of the present Sec. 3, in which the matter and graviton causal cones exactly coincide everywhere.

horizon, but it would be perfectly centered and the time axis would be inside it.

To prove stability, we also need to study spin-0 perturbations. In order to extract the effective metric in which they propagate, we focused on the $\ell = 0$ (spherically symmetric) even-parity modes, which can only describe a scalar degree of freedom. We found^{1,2} that the scalar cone has a consistent orientation with the matter and graviton cones (i.e., both a common interior and a common exterior) if and only if

$$\text{either } \eta > 0, \beta < 0 \quad \text{and} \quad \frac{\Lambda_{\text{bare}}}{3} < -\frac{\eta}{\beta} < \Lambda_{\text{bare}}, \quad (14)$$

$$\text{or } \eta < 0, \beta > 0 \quad \text{and} \quad \Lambda_{\text{bare}} < -\frac{\eta}{\beta} < 3\Lambda_{\text{bare}}. \quad (15)$$

Since Eq. 12 tells us that $\Lambda_{\text{eff}} = -\eta/\beta$, these conditions actually prove that self-tuning is impossible in the model of Eq. 10: The observed cosmological constant Λ_{eff} can never be negligible with respect to the bare one Λ_{bare} , otherwise the solution is unstable. However, this model and its solution are experimentally viable if Λ_{bare} is assumed to be small enough, like in general relativity, and Fig. 2 illustrates that it is stable when Eq. 14 is satisfied. Indeed the scalar (dashed blue) causal cone remains everywhere consistent with the matter and graviton causal cones. It is difficult to see what happens near the black-hole horizon, because this scalar causal cone opens almost totally. This is again an coordinate artifact, because we chose to plot the matter (grey) cone at $\pm 45^\circ$. This matter cone actually becomes infinitely thin near the black-hole horizon, in Schwarzschild coordinates, and our rescaling of the time coordinate in Fig. 2 is thus responsible for the wide opening of the scalar (blue) cone. But its exterior always exists, and there is thus always a common exterior to all three causal cones, where one may specify initial data.

4 Conclusions

The main message of this presentation is that a Hamiltonian density which is unbounded from below does not always imply an instability. Indeed, the 3-momentum is also conserved, and it may be linearly combined with the energy to give a bounded-by-below quantity —which actually coincides with the Hamiltonian computed in another coordinate system. The simplest way to analyze the stability of a solution is to plot the causal cones of all degrees of freedom: There should exist both a common interior and a common exterior spacelike hypersurface. This stability criterion may be expressed as a generalization of the Weak Energy Condition of general relativity, now encompassing the case of several causal cones. Finally, we illustrated this criterion by showing that an exact Schwarzschild-de Sitter solution of a Horndeski theory is stable for a given range of its parameters, contrary to a claim in the literature.

References

1. E. Babichev, C. Charmousis, G. Esposito-Farèse and A. Lehébel, *Phys. Rev. Lett.* **120**, 241101 (2018) [arXiv:1712.04398 [gr-qc]].
2. E. Babichev, C. Charmousis, G. Esposito-Farèse and A. Lehébel, *Phys. Rev. D* **98**, 104050 (2018) [arXiv:1803.11444 [gr-qc]].
3. H. Ogawa, T. Kobayashi and T. Suyama, *Phys. Rev. D* **93**, 064078 (2016) [arXiv:1510.07400 [gr-qc]].
4. K. Takahashi, T. Suyama and T. Kobayashi, *Phys. Rev. D* **93**, 064068 (2016) [arXiv:1511.06083 [gr-qc]].
5. K. Takahashi and T. Suyama, *Phys. Rev. D* **95**, 024034 (2017) [arXiv:1610.00432 [gr-qc]].
6. R. Kase, M. Minamitsuji, S. Tsujikawa and Y. L. Zhang, *JCAP* **1802**, 048 (2018) [arXiv:1801.01787 [gr-qc]].
7. Y. Aharonov, A. Komar and L. Susskind, *Phys. Rev.* **182**, 1400 (1969).

8. C. Armendariz-Picon, T. Damour and V. F. Mukhanov, *Phys. Lett. B* **458**, 209 (1999) [hep-th/9904075].
9. E. Babichev, V. F. Mukhanov and A. Vikman, *JHEP* **0609**, 061 (2006) [hep-th/0604075].
10. J.-P. Bruneton, *Phys. Rev. D* **75**, 085013 (2007) [gr-qc/0607055].
11. J.-P. Bruneton and G. Esposito-Farèse, *Phys. Rev. D* **76**, 124012 (2007) [arXiv:0705.4043 [gr-qc]].
12. E. Babichev, V. Mukhanov and A. Vikman, *JHEP* **0802**, 101 (2008) [arXiv:0708.0561 [hep-th]].
13. G. W. Horndeski, *Int. J. Theor. Phys.* **10**, 363 (1974).
14. E. Babichev and C. Charmousis, *JHEP* **1408**, 106 (2014) [arXiv:1312.3204 [gr-qc]].
15. E. Babichev and G. Esposito-Farèse, *Phys. Rev. D* **95**, 024020 (2017) [arXiv:1609.09798 [gr-qc]].
16. E. Babichev and G. Esposito-Farèse, *Phys. Rev. D* **87**, 044032 (2013) [arXiv:1212.1394 [gr-qc]].